On Realizing Distributed Topology Control in Low-power IoT Platforms

Phivos Phivou
Department of Computer Science
University of Crete, Heraklion, Greece
Email: fivou@csd.uoc.gr

Athanasia Panousopoulou
Institute of Computer Science
FORTH, Heraklion, Crete
Email: apanouso@ics.forth.gr

Panagiotis Tsakalides
Institute of Computer Science, FORTH, and
Department of Computer Science
University of Crete, Heraklion, Crete
Email: tsakalid@ics.forth.gr

***Abstract*—As current trends in distributed computing are enabling the vision of the Internet of Things (IoT), the necessity intensifies for addressing real-life aspects in massive scales. Energy efficiency remains a key design requirement for low-power IoT platforms, and distributed topology control techniques can yield the guidelines for optimizing the transmission power-connectivity nexus. In this work, we exploit previous theoretical results on necessary and sufficient conditions for establishing end-to-end connectivity, by introducing the notion of relative Delaunay neighbourhoods to computationally constrained hardware platforms. We implement the proposed approach on Contiki OS and we offer extensive emulation results, which highlight the scalability of our approach. Comparisons with benchmark solutions are offered to evaluate the performance of our framework in terms of achieved connectivity, memory demands, and energy efficiency.**

***Index Terms*—Internet of Things; Topology Control; Connectivity; Delaunay Graph; Contiki OS.**

I. Introduction

The last decade has witnessed pioneering efforts in advancing versatile network architectures that facilitate our interaction with the physical world over miniaturized, smart devices. A new field of research has emerged, coined as the Internet of Things (IoT) [1], offering advanced network services that abstract the heterogeneity in hardware, protocols, and domains.

To enable the vision of the IoT ecosystem, hundreds of low-cost, low-power embedded devices should be self-organized in connected networks, regardless of the energy and operational constraints [2], [3]. Therefore, safeguarding the autonomous character of connectivity for the network backbone is a prerequisite for advanced IoT network services, such as the Constrained Application Protocols (COAP) [4].

Connectivity can be treated as a topology control problem [5], aiming to optimize the transmission power needed for guaranteeing the existence of network links between any pair of nodes. Nevertheless, connectivity aspects are still treated at a theoretical level. For instance, the authors in [6], propose a distributed scheme for minimizing the transmission power that preserves connectivity in lossy networks. The key assumption made therein is that each node has a-priori knowledge of the reception link quality within its two-hop neighbourhood at different transmission power levels. This is considered unrealistic, especially for scalable deployments in highly dynamic environments. Hence, the question that raises is whether distributed algorithms for enabling connectivity are implementable in low-power IoT platforms, and how they would perform in scalable deployments, where nodes cannot have a global view of the entire network.

The issues addressed in this paper are related to the mechanisms that enable distributed topology control in low power IoT platforms. Our emphasis is on end-to-end connectivity, which describes the bidirectional connectivity between each pair of nodes in the network. Specifically, we extend the theoretical work presented in [7] and we propose a framework for enabling distributed topology control in IoT platforms. The key benefit of the herein proposed approach is that it eliminates the necessity of additional network traffic. A structured procedure is adopted for evaluating distributed topology control algorithms in IoT platforms against realistic factors, such as computational constraints, memory demands, and the energy needed for reaching the outcome of the algorithm. The results highlight the superiority of the proposed scheme against benchmark solutions, thereby yielding a promising approach for tackling connectivity issues.

The remainder of this paper is organized as follows: in Section II, the end-to-end connectivity problem is formulated, accompanied by an overview of the practical considerations on distributed topology control in Section III. Section IV presents the proposed framework and Section V elaborates on its evaluation. Conclusions are drawn in Section VI.

II. Problem Formulation

We consider an IoT network comprised of N operational nodes, deployed within a 2D region. Each i node is characterized by its Cartesian coordinates, and a discrete set $S_i = \{P_k | k = 1, 2, \ldots, K\}$ of K levels of transmission power P_i^{tx}, where P_1 and P_K correspond to the minimum and maximum level of transmission power, respectively. The contents of S_i may vary for different nodes, and the maximum transmission power is henceforth noted as $\rho_i^{\max}$. In addition, each node can establish peer-to-peer connections at the MAC sub-layer with the remaining nodes that are within its transmission range.

The problem at hand is the distributed calculation of the minimum transmission power per node that preserves the end-to-end connectivity. Specifically, the network is modelled as a graph $G = (V_N, E_N)$, where V_N is the set of operational nodes and E_N is the edges set, corresponding to bidirectional

connectivity links $i \leftrightarrow j$ between first-hop neighbours i and $j \in V_N$. The theoretical perspective of the graph [7] considers that the formation of the first-hop neighbourhood on each i-th node depends on the characteristics of the adopted propagation model, directly associated to the spatial configuration of the network. By contrast, the practical perspective herein addressed, considers that the first-hop neighbourhood is constructed at the MAC sub-layer, during a typical neighbour discovery mechanism, based on broadcasting. Without loss of generality we consider that each node broadcasts discovery messages, containing their 2D coordinates, at ρ_i^{max}. Any node i within their transmission range can in turn construct the set $\tilde{\Gamma}_i$ of operational nodes, defined as the set of nodes $j \in V_N$ from which it receives discovery messages.

The contents of $\tilde{\Gamma}_i$ abstract any realistic imperfection, such as the maximum transmission range limitations, network failures (e.g. collisions, packet losses, and interference), and hardware computational constraints. As a consequence, at the end of this discovery process, each node has a relative view of entire network.

From a global perspective, the connectivity of graph G depends on the intersections $\tilde{\Gamma}_i \bigcap \tilde{\Gamma}_i,\ i, j, \in V_N$. The length and contents of $\tilde{\Gamma}_i$ can be significantly reduced when each node reduces its transmission power for energy conservation purposes. As a consequence, the initial graph G would be reduced at $G^* = (V_N, E_N^*)$, where $E_N^* \subseteq E_N$. Hence, the objective for each node is to calculate the minimum transmission power ρ_i^*, such that the resulting graph G^* preserves the connectivity properties of the initial graph G.

III. Distributed Per-Node Topology Control

The formulation given in Section II describes a per-node distributed topology control problem [8]. Available benchmark approaches, such as the Local Minimum Spanning Tree (LMST) [9], consider network solutions that combine information from the first- and second-hop neighbourhoods. The access to such information allows each node i to adopt a typical MST algorithm, calculate, and apply the optimal level ρ_i^*, for constructing graph G^*. Despite their optimal theoretical performance, such approaches reflect on ideal operational conditions, as they assume network reliability during the first- and second-hop neighbourhood discovery. In addition, the memory available at each node for calculations is considered unlimited, while the energy needed for realizing the topology control approach is not taken into account.

The aforementioned assumptions introduce strong disincentives for applying such approaches in realistic, large-scale scenarios, accompanied by network imperfections. The authors in [10] argue in favour of the construction of approximated tree structures by introducing the concept of Nearest Neighbour Trees (NNT). This family of solutions suggests the dissemination of rankings between first-hop neighbours for constructing trees, much like the IEFT standard on Routing for Low Power and Lossy Networks (RPL) [11]. On a theoretical basis, it is proven that such approaches fit better the IoT paradigm than a LMST-based approach, in terms of computational, time, and message complexity. Nevertheless, the realization of an NNT-based scheme still considers two key simplifications that prevent us from adopting it in large-scale deployments. First, for the case of a multi-hop network, it assumes the existence of single sink-multiple sources network topology. Second, it heavily relies on customized messages exchange for calculating the ranking between adjacent nodes, thereby introducing a severe energy overhead as the density of the network, or equivalently the length of $\tilde{\Gamma}_i$, increases.

An alternative to the mainstream of approaches is presented in [7], [12] and exploits the properties of Delaunay triangulation [13] for extracting the sufficient network conditions that guarantee end-to-end connectivity. A Delaunay triangulation is a planar graph with the key characteristic that no vertex is within the circumcircle of any triangle. At the level of the i-th node, the vertices of the Delaunay graph that are adjacent to the i-th vertex formulate the local set $\tilde{\Delta}_i$ of Delaunay neighbours, where $\tilde{\Delta}_i \subseteq \tilde{\Gamma}_i$. In a nutshell, it is proven in [7] that if each node can construct a localized Delaunay triangulation from the contents of $\tilde{\Gamma}_i$ and if it can establish connectivity paths with its Delaunay neighbours via Delaunay edges, then end-to-end connectivity is satisfied for the entire network. The respective Relative Delaunay Connectivity Algorithm (REDELCA) calculates the minimum transmission power ρ_i^* that allows the i-th node to realize a shortest connectivity path towards each node $j \in \tilde{\Delta}_i$, at no further expense.

The discussion thus far highlights the clear advantage of REDELCA against LMST- and NNT-based topology control solutions, in terms of network overhead. As opposed to LMST and NNT, REDELCA introduces only the expense of neighbourhood discovery for applying topology control to real-life and scalable deployments. Motivated by this key characteristic, in Section IV we introduce a design framework for implementing REDELCA in IoT platforms.

IV. Enabling Per-node Topology Control

Figure 1 presents the architecture for implementing REDELCA in low-power IoT platforms, identifying the existence of three main components, namely: (a) the 1-hop neighbour Discovery component, (b) the Delaunay Triangulation component, and (c) the REDELCA component.

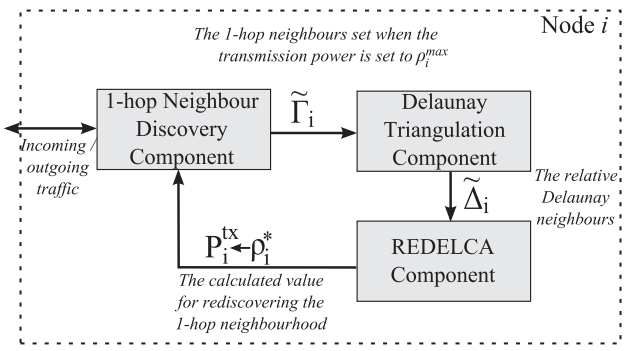

Fig. 1. The component-based architecture for implementing REDELCA.

The 1-hop Neighbour Discovery component is responsible for constructing the set $\tilde{\Gamma}_i$, which as described in Sections II -III, contains the baseline information for applying per-node topology control in a distributed fashion. To efficiently address the computational constraints met in conventional sensor platforms while taking into account link quality aspects, the length of $\tilde{\Gamma}_i$ is constrained by an upper threshold γ. Without loss of generality, the value of γ is pre-defined and directly associated to both the memory and storage capabilities of each node, as well as the quality of reception of discovery packets. Specifically, while constructing the set $\tilde{\Gamma}_i$, the i-th node ranks the nodes with respect to their Received Signal Strength Indicator (RSSI), which can provide insights on the anticipated packet reception ratio [14]. As a consequence, the set $\tilde{\Gamma}_i$ is comprised by up to γ 1st-hop neighbours j with the highest ranking in RSSI terms. The remaining 1-hop neighbours are discarded. Finally, considering that each node features its 2D-coordinates, the calculation of the set $\tilde{\Gamma}_i$ implies that the i-th node has access to the related spatial attributes of each $j \in \tilde{\Gamma}_i$.

The Delaunay Triangulation component exploits the contents of $\tilde{\Gamma}_i$ and the accompanying Cartesian coordinates for calculating the tessellation of $\tilde{\Gamma}_i \bigcup \{i\}$ into Delaunay triangles. The calculation follows the basic principles of the algorithm available at [13] and relies on the randomized incremental approach. The pseudo code therein provided suggests a master triangle consisting of the highest and right most point of $\tilde{\Gamma}_i \bigcup \{i\}$ and two additional points p_{-1}, p_{-2}, which are arbitrarily defined to form a convex hull with the rightmost and the leftmost points of the set, respectively. In order to tackle the practical difficulties of arbitrarily setting sufficiently distant coordinates for p_{-1} and p_{-2}, our proposed design considers a master triangle consisting of three external points p_{-1}, p_{-2}, p_{-3}, based on the maximum value of all coordinates in the set $\tilde{\Gamma}_i \bigcup \{i\}$. This modification is considered essential for saving both computational time and memory resources.

The calculation of the Delaunay triangulation at the side of the i-th node yields the set of Delaunay neighbours $\tilde{\Delta}_i$, which is further employed by the REDELCA component for deriving the optimal transmission power ρ_i^*. The proposed design considers the calculation of the shortest connectivity path $p_{ij} = \{i, u, \ldots, j\}$ to each Delaunay neighbour j, with $u \in \tilde{\Delta}_i$, by employing the Dijkstra algorithm. The cost function for the shortest path is related to the total transmission power needed for realizing p_{ij} over the Delaunay edges of i and it depends on two factors, namely (i) the Euclidean distance between all nodes in $\tilde{\Gamma}_i \bigcup \{i\}$, and (ii) a propagation model that links distance and signal attenuation. The calculation steps of the REDELCA component are summarized in Algorithm 1. The REDELCA component will preserve the level of transmission power $\rho_{ij} \in S_i$ that enables first-hop connectivity between i and its immediate neighbour u through the shortest path p_{ij}. The same procedure is repeated for all Delaunay neighbours and sets ρ_i^* as the maximum value over $\rho_{ij}, \forall j \in \tilde{\Delta}_i$. Upon completion of the calculations made by the REDELCA component, each node i can apply the optimal value ρ_i^* as its transmission power ($P_i^{tx} \leftarrow \rho_i^*$) and re-iterate the first-hop neighbourhood discovery process and/or any other nominal network operation.

Algorithm 1: The REDELCA component.

For each node $i \in V_N$:
Initialize the value of ρ_i^* at the minimum available value of S_i.
Require: The set of Delaunay neighbours $\tilde{\Delta}_i$ and the respective Delaunay edges.
Ensure: The value $\rho_i^* \in S_i$ of the transmission power P_i^{tx}, $\forall i \in V_N$.
for $j \in \tilde{\Delta}_i$ **do**
  Apply the Shortest Power Path Algorithm [12] and calculate the value $\rho_{ij} \in S_i$ of the transmission power that realizes the shortest path p_{ij} over the Delaunay edges of i.
  if $\rho_i^* < \rho_{ij}$ **then**
    $\rho_i^* \leftarrow \rho_{ij}$
  end if
end for

The proposed framework is adopted by each node. An example is presented in Figure 2, highlighting the lightweight, locally conducted procedures, which do not introduce additional network traffic. This is achieved at the expense of the time complexity for deriving a Delaunay triangulation out of $\tilde{\Gamma}_i$ at the i-th node, which can become significant as the network size N increases. Nevertheless, as shown in Section V, the proposed design framework can yield a robust solution for distributed per-node topology control, even when the network size becomes severely large.

V. Implementation and Evaluation Studies

The proposed framework has been implemented as a set of modules for the Contiki OS [15], which is a popular choice for IoT architectures [16]. The resulting mechanism is targeted to operate at low-cost, low-power sensor platforms, such as the Z1 platform [17]. Whilst currently implemented as a standalone application, our approach can be readily transformed to a built-in module, positioned between the MAC and Radio Duty Cycle layers of the Contiki protocol stack.

The evaluation has been made in the Cooja environment, which allows both the packet-driven emulation of the network dynamics, as well as the emulation of the hardware platform. The emulation procedure entails a wide range of network instances in a predefined 2D region and it employs 10 different cases of normal distribution on the nodes deployment per network size, where $N = \{4, 9, 14, \ldots, 199\}$. Table I summarizes the emulation parameters.

The performance of the REDELCA-based topology control is evaluated against the performance of a benchmark approach that adopts the principles of LMST. The LMST-based topology control follows the basic steps of the proposed framework in terms of first-hop neighbour (re)discovery. The key difference is that it also requires the discovery of the second-hop neighbourhood, i.e. $\tilde{\Gamma}_j$, $\forall j \in \tilde{\Gamma}_i$. This information is employed for calculating the members j, u of $\tilde{\Gamma}_i$ such that $u \in \tilde{\Gamma}_i \bigcap \tilde{\Gamma}_j$. Based on this information, the Prim algorithm is employed for calculating the MST from the i-th node towards each node

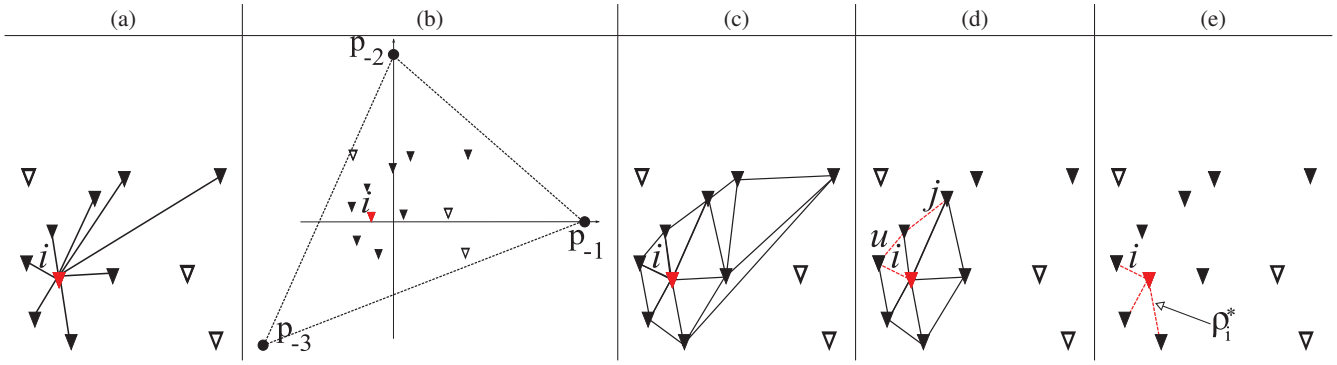

Fig. 2. The framework for enabling per-node topology control based on the REDELCA mechanism: (a) During the neighbour discovery process the i-th node builds the $\tilde{\Gamma}_i$, comprised by the ▲ nodes; (b) The $\{i\} \bigcup \tilde{\Gamma}_i$ set is considered for the on-node calculation of the Delaunay triangulation; (c) The resulting Delaunay tessellation; (d) The shorted connectivity path (red dashed line) between i and its Delaunay neighbour j, through $u \in \tilde{\Delta}_i$; (e) The direct links that the i-th node should implement in order to establish connectivity with all members of $\tilde{\Delta}_i$, indicating the link that corresponds to the optimal value ρ_i^*.

TABLE I
EMULATION PARAMETERS

Emulation Parameter	**Value**
Cooja Propagation Model	Unit Disk Graph (UDG)
Transmission Range at $\rho_i^{\max}$	15m
Contiki Protocol Stack	NullRDC, CSMA/CA, Broadcast channel
Hardware Platform	Zolertia Z1 (MCU @ 8MHz)
Current Draw at MCU / RX	4.5mA / 20mA
S_i (dBm)	{-25, -15, -10, -7, -5, -3, -1, 0}
γ	20

$j \in \tilde{\Gamma}_i$, using a cost function similar to the one employed for the proposed design framework. The resulting value for ρ_i^* is finally applied for the first-hop rediscovery process. The Contiki modules for REDELCA- and LMST-based topology control are available in [18].

A. Emulation Results

The evaluation metrics cover network and nodes' aspects. With regard to the network performance, we consider the end-to-end connectivity index, defined as the normalized number of disconnected pairs of nodes on G^*, and the normalized number of nodes that fail to produce a result due to computational failures. The evaluation at a nodal level is performed against the memory demands and the energy consumption.

1) Network-wide Evaluation: The estimated Cumulative Distribution Function (CDF) of the resulting ρ_i^* for all network cases examined is presented in Figure 3(a). The LMST-based topology control module yields better results in terms of ρ_i^* than those provided when the REDELCA-based module is applied on the network. This is expected, due to the nature of the Prim algorithm, which calculates the minimum spanning tree between each nodal pair i, j with $j \in \tilde{\Gamma}_i$. As such when applying the LMST-based solution, the i-th node will have to preserve fewer connectivity edges, and it will prefer as adjacent nodes those that optimize the received link quality-transmission power nexus. By contrast, the REDELCA-based module scheme attempts to establish connectivity over Delaunay edges, which are considered a superset of MST edges [19]. As a consequence, when applying the REDELCA-based modules, the i-th will attempt to establish more connectivity links, imposing higher levels of ρ_i^* than those calculated by the LMST-based approach.

From an energy-conservative and theoretical perspective, the lowest value of ρ_i^* yields the optimal solution. Nevertheless, this might have an impact on the connectivity index, especially as the network size N increases. This aspect is highlighted in Figure 3(b). As expected, for small values of N the connectivity at ρ_i^* is not achieved, implying that in these cases end-to-end connectivity on G^* is not achievable at the maximum allowable power. For both approaches, connectivity conditions dramatically improve as the network becomes more dense ($N \geq 24$). The end-to-end connectivity resulting from the REDELCA- and LMST-based topology control modules follows a similar course, which slightly differentiates when $N \geq 79$. In particular, when the REDELCA-based mechanism is applied, the mean value of the connectivity index remains constantly greater than 0.9984. By contrast, when the LMST mechanism is employed, the mean value of the connectivity index deteriorates, due to the combination of two factors. First, the network conditions deteriorate as the network size increases, and, subsequently, the probability of inconsistencies between the first- and second-hop neighbourhood increases. Second, the fewer connectivity options imposed by the LMST-based modules constitute the entire network less resilient to failures, thus resulting to the existence of disconnected nodes.

Another interesting aspect is the capability of each low-power IoT platform to successfully complete the topology control task. Figure 3(c) presents the estimated CDF of the normalized number of nodes per network size that fail to calculate the value ρ_i^*, due to memory errors during runtime. Representative examples of such errors are the incapability of the micro-controller to dynamically allocate memory blocks of RAM, and the incapability of the Delaunay triangulation module to produce a valid tessellation, due to, for instance, degenerate cases of spatial deployments. In these cases, the control of the program returns to the neighbourhood rediscovery process, by applying $\rho_i^* \leftarrow \rho_i^{\max}$. The REDELCA-based

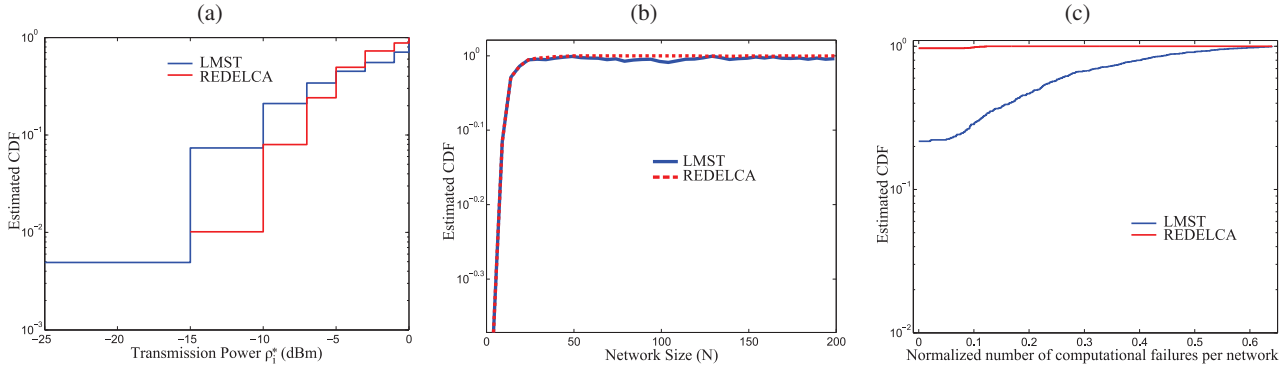

Fig. 3. Network-wide results: (a) the estimated CDF of the resulting ρ_i^*, (b) the mean value of the connectivity index versus the network size N, (c) the estimated CDF of the number of computational failures per network, when either REDELCA- or LMST-based mechanism is applied.

scheme outperforms in this practical aspect when compared to the LMST-based module. In particular, when the REDELCA-based technique is employed, it is unlikely to have a computational failure; the probability of affecting less than the 10% of the operational nodes equals to 0.995. By contrast, the increased demands in memory for handling and synchronizing 2-hop neighbours over the contents of $\tilde{\Gamma}_i$ has severe impact on the computational stability of the low-power platform. As a result, when the LMST-based module is applied, the error probability dramatically increases, and the possibility of affecting more than the 10% of the network equals to 0.685.

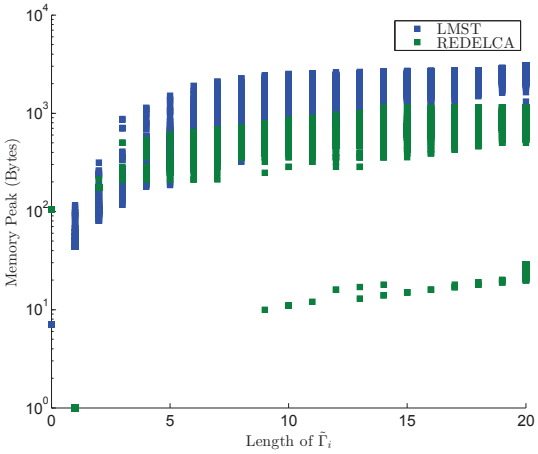

Fig. 4. The memory peak per node versus the length of $\tilde{\Gamma}_i$ for all network instances examined.

2) Evaluation per node: Figure 4 presents the memory peak per node versus the length of $\tilde{\Gamma}_i$ for all network cases examined. As expected, increasing the number of first-hop neighbours results to an increase of the memory peak per node when either the REDELCA- or the LMST-based scheme is employed. Nevertheless, it is interesting to observe that the REDELCA-based module is far less demanding in terms of RAM memory than the LMST-based modules; when $\left|\tilde{\Gamma}_i\right| \geq 5$, the REDELCA-based modules require 50% less RAM size than the one needed by the LMST-based modules. This behavior highlights the lightweight character of the REDELCA-based module, which relies on a single linked list for storing all Delaunay triangles and performing all calculations. By contrast, the implementation of the LMST-based scheme on the i-th node requires separated lists both for storing the contents of $\tilde{\Gamma}_j$, as well as for calculating and processing the intersections $\tilde{\Gamma}_j \bigcap \tilde{\Gamma}_i$, $\forall j \in \tilde{\Gamma}_i$.

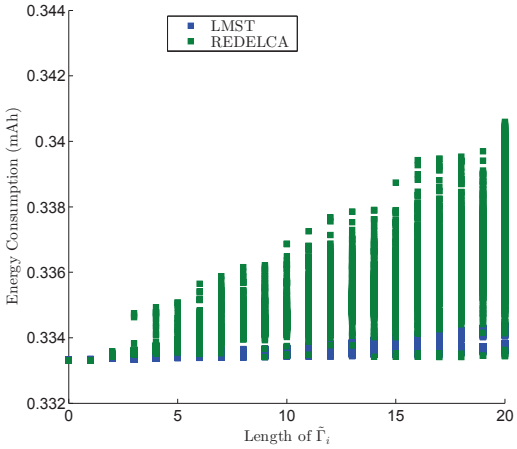

Fig. 5. The energy consumption versus the length of $\tilde{\Gamma}_i$ for all network instances examined.

Figure 5 presents the energy consumption per node for calculating the value ρ_i^*, while excluding the network overhead introduced by the first- and second-hop neighbourhood (re)discovery procedures. The increase of the network size has an impact on the energy demands, due to the respective increase of $\left|\tilde{\Gamma}_i\right|$. Overall, the LMST-based scheme offers a more energy conservative method for calculations than the REDELCA-based modules. However, the energy gap is not severe, since the difference in consumption does not exceed 0.0062mAh for all cases emulated. In addition, we observe the deviation in the energy consumption across the examined cases of network size is smaller when the LMST-based scheme is employed than when the REDELCA-scheme is applied. The

TABLE II
THE MEAN ENERGY CONSUMPTION PER MODULE ON Z1 PLATFORM

REDELCA	LMST	LMST Overhead (2-hop neigh/hood discovery)
0.337mAh	0.334mAh	0.667mAh

difference between sparse ($\left|\tilde{\Gamma}_i\right|$ =0) and dense ($\left|\tilde{\Gamma}_i\right|$ =20) 1-hop neighbourhoods does not exceed 0.0014mAh when the LMST-based scheme is employed, as opposed to 0.0076mAh, which is observed when the REDELCA module is applied. This is due to the fact that the energy consumption depends on the time needed for calculation. Figure 6 highlights the relationship between the size of Delaunay triangulation, in terms of Delaunay triangles, and the CPU time for calculating ρ_i^*. The linear dependency therein presented is a result of the memory-conservative implementation style of the REDELCA-based module, which considers a single linked list for all Delaunay-related calculations. As such, during the calculation of ρ_i^*, the i-th node scans the entire set of Delaunay triangles for valid neighbours (i.e. $\tilde{\Delta}_i$), instead of creating and processing a separated memory structure for $\tilde{\Delta}_i$.

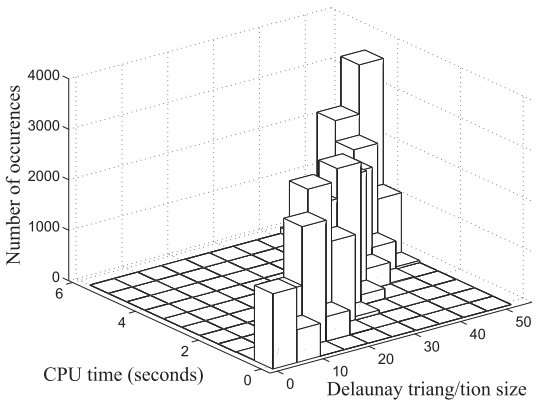

Fig. 6. The Delaunay triangulation size versus the calculation time per node.

Another important energy-related aspect is the network overhead. Table II summarizes the energy consumption per calculation module, and presents the energy consumption overhead of the LMST-based module due to the 2-hop neighbourhood discovery, which equals to 0.667mAh. Hence, the overall value of energy consumption equals to 1mAh when the LMST-based module is applied, as opposed to 0.337mAh which is the respective value for the REDELCA-based scheme.

VI. CONCLUSIONS AND FUTURE WORK

In this work, the realization of per-node topology control has been addressed for low-power IoT platforms. A design framework, adopting a purely localized approach that allows each node to calculate the transmission power required to establish end-to-end connectivity has been presented and implemented in Contiki OS. A rigorous emulation procedure was employed, and the results highlighted the efficacy of the proposed scheme against mainstream approaches, in terms of achieved connectivity, memory demands, and energy consumption.

The transition to mobile deployments will form the basis of our future work. In addition, the extensions towards emerging IoT aspects, such as Radio Duty Cycle, are considered extremely interesting. We envisage that the respective challenges for real-time adaptation , will yield the opportunity to further extend the functionalities of the herein proposed framework towards an integrated set of tools for enabling the IoT vision.

ACKNOWLEDGEMENTS

This research has been co-financed by the European Union and Greek national funds through the National Strategic Reference Framework (NSRF), Research Funding Program: Cooperation-2011, Project SeNSE.

REFERENCES

[1] A. Bassi, M. Bauer, M. Fiedler, T. Kramp, R. van Kranenburg, S. Lange, and S. Meissner, *Enabling things to talk*. Springer, 2013.
[2] D. Miorandi, S. Sicari, F. D. Pellegrini, and I. Chlamtac, "Internet of things: Vision, applications and research challenges," *Ad Hoc Networks*, vol. 10, no. 7, pp. 1497 – 1516, 2012.
[3] A. Zanella, N. Bui, A. Castellani, L. Vangelista, and M. Zorzi, "Internet of things for smart cities," *Internet of Things Journal, IEEE*, vol. 1, no. 1, pp. 22–32, Feb 2014.
[4] M. Kovatsch, M. Lanter, and Z. Shelby, "Californium: Scalable cloud services for the internet of things with coap," in *Internet of Things (IOT), 2014 International Conference on the*, Oct 2014, pp. 1–6.
[5] M. Li, Z. Li, and A. Vasilakos, "A survey on topology control in wireless sensor networks: Taxonomy, comparative study, and open issues," *Proceedings of the IEEE*, vol. 101, no. 12, pp. 2538–2557, 2013.
[6] G. Xing, C. Lu, X. Jia, and R. Pless, "Localized and configurable topology control in lossy wireless sensor networks," *Ad Hoc Networks*, vol. 11, no. 4, pp. 1345 – 1358, 2013.
[7] A. Panousopoulou, R. Sterritt, and A. Tzes, "Localised transmission power adjustment for relative connectivity awareness in wireless ad-hoc amp; sensor networks," in *American Control Conference (ACC), 2012*, June 2012, pp. 460–465.
[8] P. Santi, "Topology control in wireless ad hoc and sensor networks," *ACM Comput. Surv.*, vol. 37, no. 2, pp. 164–194, Jun. 2005.
[9] N. Li, J. Hou, and L. Sha, "Design and analysis of an mst-based topology control algorithm," *Wireless Communications, IEEE Transactions on*, vol. 4, no. 3, pp. 1195–1206, May 2005.
[10] M. Khan, G. Pandurangan, and V. S. Anil Kumar, "Distributed Algorithms for Constructing Approximate Minimum Spanning Trees in Wireless Sensor Networks," *IEEE Transactions on Parallel and Distributed Systems*, vol. 20, no. 1, pp. 124–139, 2009.
[11] *Routing Protocol for Low Power and Lossy Networks*, IEFT Std., 2011. [Online]. Available: http://tools.ietf.org/html/draft-ietf-roll-rpl-19
[12] A. Panousopoulou and A. Tzes, "Rf-power overlapping control for connectivity awareness in wireless ad-hoc and sensor networks," in *2nd IFAC Workshop on Distributed Estimation and Control in Networked Systems (NecSys 2010)*, 2010, pp. 275–280.
[13] M. De Berg, M. Van Kreveld, M. Overmars, and O. C. Schwarzkopf, *Computational geometry*. Springer, 2000.
[14] K. Srinivasan, P. Dutta, A. Tavakoli, and P. Levis, "An empirical study of low-power wireless," *ACM Trans. Sen. Netw.*, vol. 6, no. 2, pp. 16:1–16:49, Mar. 2010.
[15] *The Contiki Operating System: Version 2.6*, 2012. [Online]. Available: http://www.contiki-os.org/start.html
[16] M. Fazio, M. Paone, A. Puliafito, and M. Villari, "Heterogeneous sensors become homogeneous things in smart cities," in *Innovative Mobile and Internet Services in Ubiquitous Computing (IMIS), 2012 Sixth International Conference on*, July 2012, pp. 775–780.
[17] "Zolertia z1 module," http://zolertia.io/z1, 2014.
[18] https://github.com/apanouso/contiki-topology-control, 2015.
[19] C. D. Toth, J. O'Rourke, and J. E. Goodman, *Handbook of discrete and computational geometry*. CRC press, 2004.